Evaluation of non-linear convection aspect to analyze Rate type chemically reacted fluid considering Cattaneo-Christov dual diffusive model

S. Z. Abbas

School of Mathematics and Statistics, Beijing Institute of Technology, Beijing 100081, China

*Corresponding author E-mail: abbas@bit.edu.cn

Abstract: The simultaneous evaluation of heat/mass transference procures momentous significance in polymer industry and engineering activities. Extensive utilizations of such aspects include propylene flares, heat exchangers, energy transfiguration in chilling towers and amputation of post fortuitous heat in nuclear reactors. Owing to such prospective demands, we interpreted the Jeffrey liquid reactive flow under non-linear convection. We scrutinized the transference of heat/mass under generalized Fourier-Fick relations. Thermal conductivity depends on temperature while mass diffusivity is dependent on concentration. Besides, heat source along with first-order chemical reaction aspects are accounted. Relevant transformations are exerted to achieve non-linear differential systems which are solved through homotopy scheme. Influences of divers factors are exhibited via graphical benchmark.

Keywords: Generalized Fourier-Fick laws; Chemical reaction; Jeffrey material; Heat source; Variable thermal conductivity; Nonlinear convection; Variable mass diffusivity.

1 Introduction

Flow analysis subjected to mixed convection has vital contribution in numerous engineering systems for illustration electronic equipment's, solar collectors and heat exchangers [1]. The mixed convected flow turn out to be more substantial when temperature-dependent buoyancy force between solid surface and free-stream become larger, which ultimately influence both

 doi:10.20944/preprints202007.0657.v1

thermal and flow fields significantly. Several investigations featuring mixed convection aspects have been elaborated by researchers under various assumptions. For instance, Waqas et al. [2] evaluated micropolar material dissipative flow employing homotopy scheme. They further accounted mixed convection along with Robin's condition in this research. Chemically reacted Casson nanomaterial dissipative flow under buoyancy forces and hydromagnetic aspects is formulated by Ibrahim et al. [3]. Irfan et al. [4] addressed mixed convection features in radiative Carreau nanoliquid stretching flow under activation energy. Robin's condition effectiveness in buoyancy-driven stratified nanomaterial flow is elucidated by Waqas et al. [5].

The heat transportation phenomenon is yielded via movement of thermal energy from one entity to an-other entity owing to temperature variation. Such entities can be liquid, gas or solid, or inside a liquid or gas. The fascination towards transportation of heat is rising noticeably owing to its copious technological and industrial demands. Extensive demands of heat transportation can be viewed in abundant engineering and industrial activities. The most advantageous demands are energy production, cooling process and fuel cells in distinct atomic mechanisms. To foresee heat transportation, Fourier's [6] introduced an effectual model to foresee heat transportation characteristics. The surprising attribute of this liquid model includes macroscopic systems analysis. Besides, the modeling subjected to Fourier's model outcomes energy expression having parabolic nature. Cattaneo [7] proposed the generality of this concept via relaxation time addition which converts Fourier's energy expression into hyperbolic type. This formula permits the heat transportation via thermal waves having restricted speed. Later, Christov [8] modified [7] via upper convected type derivative replacement with usual derivative appearing in it. Few researches under Cattaneo-Christov model of heat transportation are given in Refs. [9-18].

Indeed various simulation algorithms are utilized for non-linear analysis. Here, we opted

Preprints (www.preprints.org) | NOT PEER-REVIEWED | Posted: 27 July 2020 doi:10.20944/preprints202007.0657.v1

homotopy scheme [19] for computational analysis.

2 Formulation

An incompressible non-linear convective Jeffrey material stretching flow is modeled. The generalized laws (Fourier-Fick) are accounted for heat/mass transportation. Thermal conductivity depends on temperature while mass diffusivity is dependent on concentration. Besides, heat source along with first-order chemical reaction aspects are accounted. The governing 2D expressions under aforesaid aspects are:

$$\frac{\partial u}{\partial x}+\frac{\partial v}{\partial y}=0, \tag{1}$$

$$u\frac{\partial u}{\partial x}+v\frac{\partial u}{\partial y}=\frac{\nu}{1+\lambda_1}\left[\frac{\partial^2 u}{\partial y^2}+\lambda_2\left(\frac{\partial u}{\partial y}\frac{\partial^2 u}{\partial x\partial y}+u\frac{\partial^3 u}{\partial x\partial y^2}-\frac{\partial u}{\partial x}\frac{\partial^2 u}{\partial y^2}+v\frac{\partial^3 u}{\partial y^3}\right)\right]$$
$$+g\left(\Omega_1(T-T_\infty)+\Omega_2(T-T_\infty)^2+\Omega_3(C-C_\infty)+\Omega_4(C-C_\infty)^2\right), \tag{2}$$

$$u\frac{\partial T}{\partial x}+v\frac{\partial T}{\partial y}+\lambda_T\begin{pmatrix}u\frac{\partial u}{\partial x}\frac{\partial T}{\partial x}+v\frac{\partial v}{\partial y}\frac{\partial T}{\partial y}+v\frac{\partial u}{\partial y}\frac{\partial T}{\partial x}\\+2uv\frac{\partial^2 T}{\partial x\partial y}+u^2\frac{\partial^2 T}{\partial x^2}\\+v^2\frac{\partial^2 T}{\partial y^2}-\frac{Q}{\rho c_p}\left(u\frac{\partial T}{\partial x}+v\frac{\partial T}{\partial y}\right)\end{pmatrix}$$
$$=\frac{1}{\rho c_p}\frac{\partial}{\partial y}\left(K(T)\frac{\partial T}{\partial y}\right)+\frac{Q}{\rho c_p}(T-T_\infty), \tag{3}$$

$$u\frac{\partial C}{\partial x}+v\frac{\partial C}{\partial y}+\lambda_C\begin{pmatrix}u\frac{\partial u}{\partial x}\frac{\partial C}{\partial x}+v\frac{\partial v}{\partial y}\frac{\partial C}{\partial y}+v\frac{\partial u}{\partial y}\frac{\partial C}{\partial x}\\+2uv\frac{\partial^2 C}{\partial x\partial y}+u^2\frac{\partial^2 C}{\partial x^2}+v^2\frac{\partial^2 C}{\partial y^2}\end{pmatrix}$$
$$+\lambda_C\left(u\frac{\partial C}{\partial x}+v\frac{\partial C}{\partial y}\right)=\frac{\partial}{\partial y}\left(D(C)\frac{\partial C}{\partial y}\right)-k_1(C-C_\infty), \tag{4}$$

$$u=u_w(x)=cx,\ v=0,\ T=T_w,\ C=C_w \text{ at } y=0,$$
$$u\to 0,\ T\to T_\infty,\ C\to C_\infty \text{ when } y\to\infty. \tag{5}$$

Here λ_2 illustrates relaxation time, ρ liquid density, (Ω_2,Ω_1) linear (solutal, thermal) expansion coefficients, Q heat source coefficient, λ_1 relationship between

Preprints (www.preprints.org) | NOT PEER-REVIEWED | Posted: 27 July 2020 doi:10.20944/preprints202007.0657.v1

relaxation/retardation times, λ_C and λ_T mass and heat flux relaxation times, c_p specific heat, T and C fluid temperature and concentration , (Ω_4, Ω_3) nonlinear (solutal, thermal) expansion coefficients, k_1 reaction rate, T_∞ and C_∞ ambient fluid temperature and concentration and u and v velocities of fluid in horizontal and vertical directions respectively and c stretching rate.

Expressions of variable diffusivity $D(C)$ along with variable conductivity $K(T)$ are:

$$D(C) = D_\infty \left(1 + \varepsilon_2 \frac{C - C_\infty}{C_w - C_\infty}\right), \tag{6}$$

$$K(T) = K_\infty \left(1 + \varepsilon_1 \frac{T - T_\infty}{T_w - T_\infty}\right), \tag{7}$$

in which (D_∞, K_∞) elucidate ambient liquid (mass diffusivity, thermal conductivity) and $(\varepsilon_2, \varepsilon_1)$ smaller parameters elaborating concentration and temperature characteristics for solutal and thermal dependent diffusivity and conductivity.

Utilizing:

$$\eta = y\sqrt{\frac{c}{\nu}},\ u = cxf'(\eta),\ v = -\sqrt{c\nu}\, f(\eta),$$
$$\theta(\eta) = \frac{T - T_\infty}{T_w - T_\infty},\ \varphi(\eta) = \frac{C - C_\infty}{C_w - C_\infty}, \tag{8}$$

Eq. (1) is authenticated mechanically whereas Eqs. (2) – (5) are:

$$f''' + (1+\lambda_1)\left(ff'' - f'^2\right) + \beta\left(f''^2 - ff^{iv}\right) + \delta(1+\lambda_1)\begin{bmatrix}(1+\beta_t\theta)\theta \\ +N(1+\beta_t\phi)\phi\end{bmatrix} = 0, \tag{9}$$

$$f(0) = 0,\ f'(0) = 1,\ f'(\infty) \to 0, \tag{10}$$

$$(1+\varepsilon_1\theta)\theta'' + \varepsilon_1\theta'^2 + \Pr f\theta' + \Pr\delta\theta - \Pr\delta\gamma_1 f\theta' - \Pr\gamma_1\left(ff'\theta' + f^2\theta''\right) = 0, \tag{11}$$

$$\theta(0) = 1,\ \theta(\infty) \to 0, \tag{12}$$

Preprints (www.preprints.org) | NOT PEER-REVIEWED | Posted: 27 July 2020 doi:10.20944/preprints202007.0657.v1

$$\left(1+\varepsilon_2\phi\right)\phi"+\varepsilon_2\phi'^2+Sc\left(f\phi'-\sigma\phi\right)+Sc\gamma_2\left(\sigma f\phi'-ff'\phi'-f^2\phi"\right)=0, \tag{13}$$

$$\phi(0)=1,\ \phi(\infty)\to 0. \tag{14}$$

With

$$\left.\begin{aligned}
&\beta=\lambda_2 c\to \text{ Deborah number}\\
&\lambda=\frac{Gr_x}{\mathrm{Re}_x^2}\to \text{thermal buoyancy variable}\\
&N=\frac{Gr_x^*}{Gr_x}\to \text{ratio of solutal to thermal buoyancy}\\
&Gr_x=\frac{g\Omega_1\left(T_w-T_\infty\right)x^3}{\nu^2}\to \text{thermal Grashof number}\\
&\mathrm{Re}_x=\frac{xu_w(x)}{\nu}\to \text{Reynolds number}\\
&Gr_x^*=\frac{g\Omega_3\left(C_w-C_\infty\right)x^3}{\nu^2}\to \text{solutal Grashof number}\\
&\beta_t=\frac{\Omega_2\left(T_w-T_\infty\right)}{\Omega_1}\to \text{nonlinear thermal convection variable}\\
&\beta_c=\frac{\Omega_4\left(C_w-C_\infty\right)}{\Omega_3}\to \text{nonlinear solutal convection variable}\\
&\mathrm{Pr}=\frac{\mu c_p}{K_\infty}\to \text{Prandtl number}\\
&S=\frac{Q}{c\rho c_p}\to \text{heat source parameter}\\
&\gamma_1=\lambda_T c\to \text{thermal relaxation parameter}\\
&\gamma_2=\lambda_C c\to \text{solutal relaxation parameter}\\
&\sigma=\frac{k_1}{c}\to \text{chemical reaction parameter}\\
&\sigma>0\to \text{destructive chemical reaction parameter}\\
&\sigma<0\to \text{generative chemical reaction parameter}\\
&Sc=\frac{\nu}{D_\infty}\to \text{Schmidt number}
\end{aligned}\right\},$$

The dimensionless drag-force $\left(C_{f_x}\,\mathrm{Re}_x^{1/2}\right)$ is expressed as:

$$\frac{1}{2}C_{f_x}\,\mathrm{Re}_x^{1/2}=\left(1+\beta\right)f"(0). \tag{15}$$

Preprints (www.preprints.org) | NOT PEER-REVIEWED | Posted: 27 July 2020 doi:10.20944/preprints202007.0657.v1

It is important to mention that computations for Nusselt along with Sherwood numbers are not possible. In fact heat-mass fluxes subjected to non-Fourier-Fick situations are not obtainable in explicit form. Thus Nusselt along with Sherwood numbers computations in non-Fourier-Fick situations are not possible.

3 Computational algorithm and convergence

We applied homotopy process [19] for nonlinear computational analysis. In this process, $\hbar$ *-curves* are essential for confirmation of convergence. As a consequence we unveiled $\hbar$*-curves* in Fig. 1. Flat parts in this figure ease to achieve acceptable estimations of auxiliary variables $\left(\hbar_f, \hbar_\theta, \hbar_\phi\right)$. We detected $-1.30 \le \hbar_f \le -0.25$, $-1.40 \le \hbar_\theta \le -0.25$ and $-1.35 \le \hbar_\phi \le -0.25$ with $\delta = \beta_t = \varepsilon_1 = \beta_c = S = \varepsilon_2 = \sigma = 0.1$, $\gamma_1 = N = \gamma_2 = 0.2$, $\beta = 0.4$, $\lambda_1 = N = 0.5$, $Sc = 0.8$ and $\Pr = 1.0$. Furthermore, convergence is established iteratively (see Table 1). Clearly Eqs. $\left(9,\ 11,\ 13\right)$ converge at *25th* order approximations.

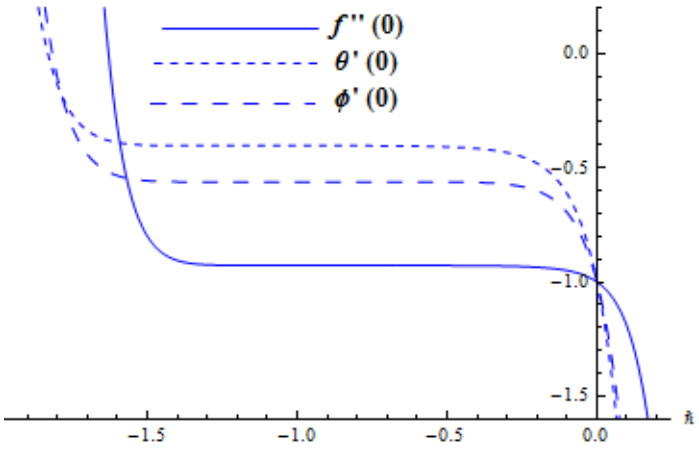

Fig. 1. $\hbar$ – curves for f, θ and ϕ.

Preprints (www.preprints.org) | NOT PEER-REVIEWED | Posted: 27 July 2020 doi:10.20944/preprints202007.0657.v1

Table 1: Convergence scrutiny for diverse order approximations considering $\delta = \beta_t = \varepsilon_1 = \beta_c = S = \varepsilon_2 = \sigma = 0.1,\ \gamma_1 = N = \gamma_2 = 0.2,\ \beta = 0.4,\ \lambda_1 = N = 0.5,\ Sc = 0.8$ and $\Pr = 1.0.$

Order of approximations	$-f''(0)$	$-\theta'(0)$	$-\phi'(0)$
1	0.9580	0.7080	0.7648
5	0.9321	0.4450	0.5768
10	0.9282	0.4097	0.5627
15	0.9280	0.4046	0.5625
20	0.9278	0.4041	0.5622
25	0.9278	0.4041	0.5622
30	0.9278	0.4041	0.5622

4 Analysis

This fragment accentuates the notable aspects of appearing variables versus velocity field $\left(f'(\eta)\right)$, concentration field $\left(\phi(\eta)\right)$ and skin-friction $\left(C_{f_x}\,\mathrm{Re}_x^{1/2}\right)$. Since we have extended the analysis of [14], therefore we scrutinized the characteristics of those variables which arises through the consideration of non-linear convection and chemical reaction. In view of that, Figs. $2-10$ are delineated and described. The change in $f'(\eta)$ curves against δ is evaluated through Fig. 2. Clearly $f'(\eta)$ curves are augmented because of δ increment. Physically, buoyancy force appears in expression of δ and higher δ yields sturdier buoyancy force. Actually such sturdier buoyancy aspect creates a force within liquid flow which leads towards larger $f'(\eta)$. From Fig. 3, we have scrutinized that larger β_t lead towards sturdier momentum boundary-layer. Indeed, difference between temperatures (wall and ambient) upsurges for higher

Preprints (www.preprints.org) | NOT PEER-REVIEWED | Posted: 27 July 2020 doi:10.20944/preprints202007.0657.v1

β_t which yields increment in $f'(\eta)$. The attributes of N on $f'(\eta)$ are portrayed in Fig. 4. We found higher $f'(\eta)$ subject to enhance N. Since N encompasses buoyancy forces (solutal and thermal). In fact solutal buoyancy force upsurges when N is increased which ultimate upsurges $f'(\eta)$. Fig. 5 reports β_c features on $f'(\eta)$. As anticipated $f'(\eta)$ enlarges when β_c is enlarged. Actually, difference between concentrations (wall and ambient) rises for larger β_c which yields $f'(\eta)$ augmentation. Figs. 6 and 7 depict σ influence on $\phi(\eta)$. Obviously liquid concentration boosts with the escalation of $\sigma > 0$. On the other hand, it dwindles for $\sigma < 0$. Actually a rise in $\sigma > 0$ communicates higher destructed reaction rate which disperses material specie efficiently. For that reason, $\phi(\eta)$ rises. In the same way, higher $\sigma < 0$ values imparts towards larger generated reaction rate which creates the material specie effectively. Hence, $\phi(\eta)$ diminishes. Fig. 8-10 highlight $\lambda_1, \beta, \delta, \beta_t, N$ and β_c influences against $C_{f_x}\,\mathrm{Re}^{1/2}$. As anticipated, $C_{f_x}\,\mathrm{Re}^{1/2}$ increases when β is enlarged. On the other hand, antithesis effects are seen for $\delta, \lambda_1, \beta_t, N$ and β_c.

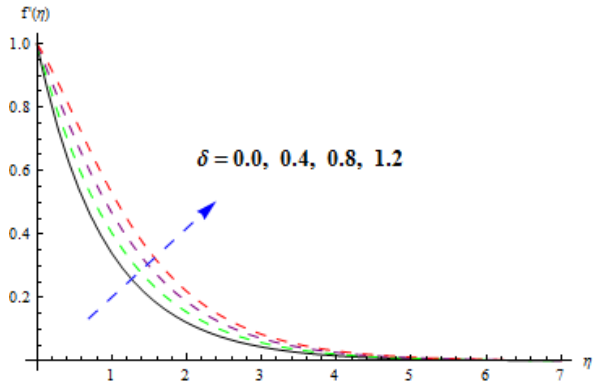

Fig. 2. δ versus $f'(\eta)$.

Preprints (www.preprints.org) | NOT PEER-REVIEWED | Posted: 27 July 2020 doi:10.20944/preprints202007.0657.v1

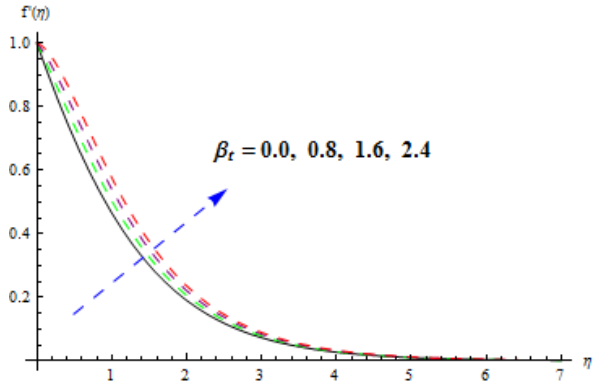

Fig. 3. β_t versus $f'(\eta)$.

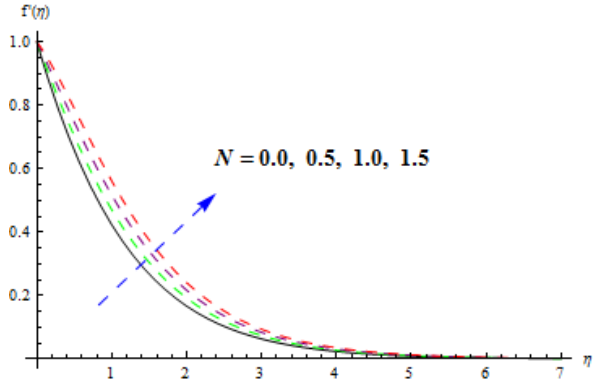

Fig. 4. N versus $f'(\eta)$.

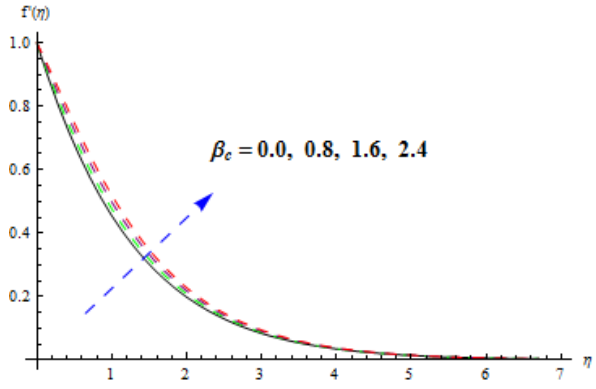

Fig. 5. β_c versus $f'(\eta)$.

Preprints (www.preprints.org) | NOT PEER-REVIEWED | Posted: 27 July 2020 doi:10.20944/preprints202007.0657.v1

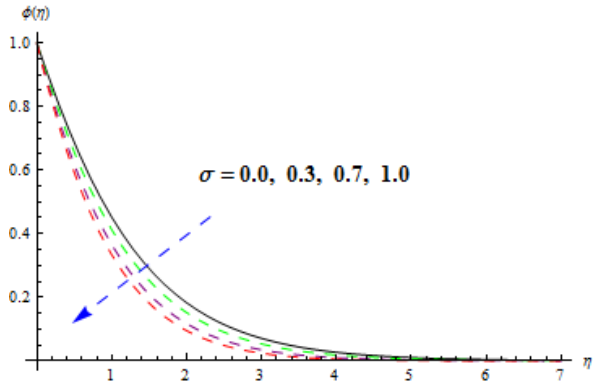

Fig. 6. $\sigma > 0$ versus $\phi(\eta)$.

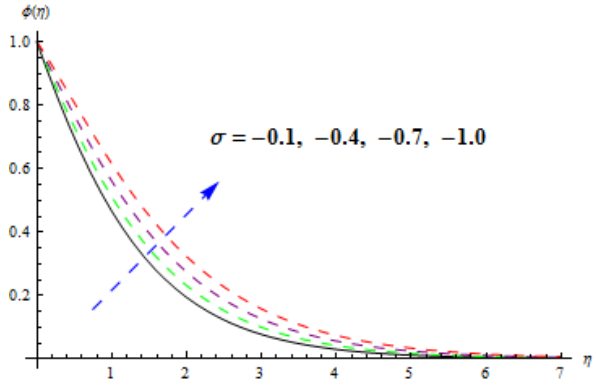

Fig.7. $\sigma < 0$ versus $\phi(\eta)$.

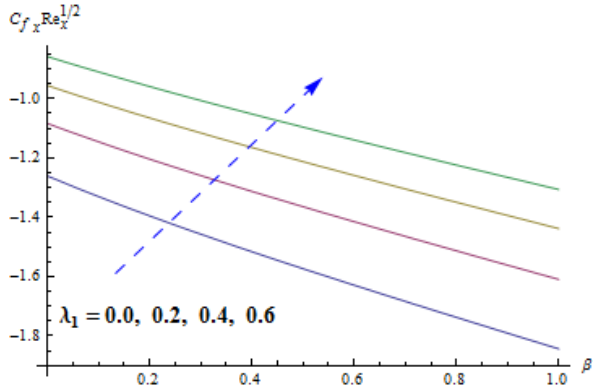

Fig. 8. λ_1 and β versus $C_{f_x}\,\mathrm{Re}^{1/2}$.

Preprints (www.preprints.org) | NOT PEER-REVIEWED | Posted: 27 July 2020 doi:10.20944/preprints202007.0657.v1

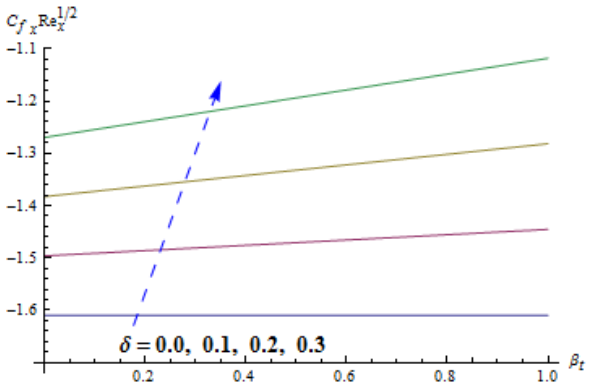

Fig. 9. δ and β_t versus $C_{f_x}\,\mathrm{Re}^{1/2}$.

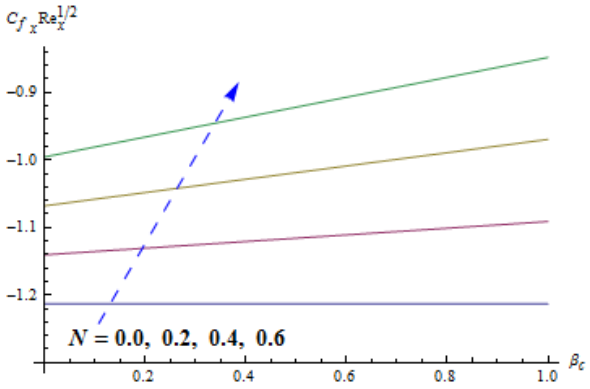

Fig. 10. N and β_c versus $C_{f_x}\,\mathrm{Re}^{1/2}$.

5 Concluding remarks

This letter discloses non-linear convective Jeffrey material stretching flow under variable diffusivity and conductivity. Heat/mass transfer account heat source, generalized Fourier-Fick expressions and chemical reaction. The abovementioned analysis leads to following conclusions:

- Velocity field $f'(\eta)$ rises when δ, β_t, N and β are increased.
- Destructive chemical reaction parameter $(\sigma > 0)$ yields higher $\phi(\eta)$ in comparison to

generative chemical reaction parameter $(\sigma < 0)$.

- Influences of δ, β_t, N and β on $f'(\eta)$ and $C_{f_x}\,\mathrm{Re}^{1/2}$ are opposite.
- The traditional Fourier-Fick expressions can be achieved by putting $\gamma_1 = 0 = \gamma$ in Eqs. (11) and (13).
- The considered fluid model reduces to viscous liquid when $\lambda_1 = 0 = \beta$.

Declaration of Interest Statement

It is declared that author has no conflict of interest.

References

1. H. Rosali, A. Ishak, R. Nazar and I. Pop, Mixed convection boundary layer flow past a vertical cone embedded in a porous medium subjected to a convective boundary condition, Propulsion and Power Research 5 (2016) 118-122.
2. M. Waqas, M. Farooq, M. Ijaz Khan, A. Alsaedi, T. Hayat and T. Yasmeen, Magnetohydrodynamic (MHD) mixed convection flow of micropolar liquid due to nonlinear stretched sheet with convective condition, International Journal of Heat and Mass Transfer 102 (2016) 766-772.
3. S. M. Ibrahim, G. Lorenzini, P. V. Kumar and C. S. K. Raju, Influence of chemical reaction and heat source on dissipative MHD mixed convection flow of a Casson nanofluid over a nonlinear permeable stretching sheet, International Journal of Heat and Mass Transfer 111 (2017) 346-355.
4. M. Irfan, W. A. Khan, M. Khan and M. M. Gulzar, Influence of Arrhenius activation energy in chemically reactive radiative flow of 3D Carreau nanofluid with nonlinear mixed convection, Journal of Physics and Chemistry of Solids 125 (2019) 141-152.

5. M. Waqas, M. I. Khan, T. Hayat, M. M. Gulzar and A. Alsaedi, Transportation of radiative energy in viscoelastic nanofluid considering buoyancy forces and convective conditions, Chaos, Solitons & Fractals 130 (2020) 109415.
6. J. B. J. Fourier, Theorie analytique De La chaleur, Paris (1822).
7. C. Cattaneo, Sulla conduzione del calore, Atti Semin. Mat. Fis. Univ. Modena Reggio Emilia 3 (1948) 83-101.
8. C. I. Christov, On frame indifferent formulation of the Maxwell-Cattaneo model of finite speed heat conduction, Mechanics Research Communications 36 (2009) 481-486.
9. B. Straughan, Thermal convection with the Cattaneo-Christov model, International Journal of Heat and Mass Transfer 53 (2010) 95-98.
10. M. Khan and W. A. Khan, Three-dimensional flow and heat transfer to burgers fluid using Cattaneo-Christov heat flux model, Journal of Molecular Liquids 221 (2016) 651-657.
11. J. V. R. Reddy, V. Sugunamma and N. Sandeep, Cross diffusion effects on MHD flow over three different geometries with Cattaneo-Christov heat flux, Journal of Molecular Liquids 223 (2016) 1234-1241.
12. A. S. Dogonchi and D. D. Ganji, Impact of Cattaneo--Christov heat flux on MHD nanofluid flow and heat transfer between parallel plates considering thermal radiation effect, Journal of the Taiwan Institute of Chemical Engineers 80 (2017) 52-63.
13. B. Mahanthesh, B. J. Gireesha and C. S. K. Raju, Cattaneo-Christov heat flux on UCM nanofluid flow across a melting surface with double stratification and exponential space dependent internal heat source, Informatics in Medicine Unlocked 9 (2017) 26-34.
14. N. Acharya, K. Das and P. K. Kundu, Cattaneo-Christov intensity of magnetised upper-convected Maxwell nanofluid flow over an inclined stretching sheet: A generalised

Fourier and Fick's perspective, International Journal of Mechanical Sciences 130 (2017) 167-173.

15. M. Irfan, M. Khan and W. A. Khan, Interaction between chemical species and generalized Fourier's law on 3D flow of Carreau fluid with variable thermal conductivity and heat sink/source: A numerical approach, Results in Physics 10 (2018) 107-117.
16. M. Shen, S. Chen and F. Liu, Unsteady MHD flow and heat transfer of fractional Maxwell viscoelastic nanofluid with Cattaneo heat flux and different particle shapes, Chinese Journal of Physics 56 (2018) 1199-1211.
17. D. H. Doh, G. R. Cho, E. Ramya and M. Muthtamilselvan, Cattaneo-Christov heat flux model for inclined MHD micropolar fluid flow past a non-linearly stretchable rotating disk, Case Studies in Thermal Engineering 14 (2019) 100496.
18. M. Sohail, R. Naz and S. I. Abdelsalam, Application of non-Fourier double diffusions theories to the boundary-layer flow of a yield stress exhibiting fluid model, Physica A: Statistical Mechanics and its Applications 537 (2020) 122753.
19. S. Liao, Homotopic analysis method in nonlinear differential equations, Springer, Heidelberg, Germany, (2012).